

Investigation on die wear behaviour during compaction of aluminium matrix composite powders

W. Li^{*1}, S. J. Park², P. Suri³, A. Antonyraj² and R. M. German¹

The focus of the current study was to evaluate and quantify the effects of particle reinforcements and lubricants on the die wear during compaction of Al matrix composites. A new wear model was developed and combined with experiments to quantify die wear using automatic die compaction experiments. The influences of the reinforcement particle type and content, as well as the premixed lubricant content, are presented and discussed.

Keywords: Aluminium, Composite powder, Compaction, Die wear

Introduction

Aluminium matrix composites (AMC) are materials consisting of a matrix of an aluminium alloy combined with a ceramic (oxide and carbide) or metallic (lead, tungsten and molybdenum) dispersed phase. Matrices of AMC are usually based on Al–Si alloys and on the alloys of 2xxx and 6xxx series. Particulate composites, long and short fibre reinforced composites are the most commonly used reinforcement phases.^{1,2} The most attractive properties include high strength at moderately elevated temperatures, high stiffness, low density, high thermal conductivity, low coefficient of thermal expansion as well as excellent wear resistance. Aluminium matrix composites are used for automotive components, brake rotors for high speed trains, bicycles, golf clubs, electronic substrates and cores for high voltage electrical cables.^{1,3}

A large portion of AMC materials are manufactured by powder metallurgy techniques, including isostatic compaction and sintering, or liquid metal infiltration of porous ceramic preforms.^{3,4} Powder metallurgy method usually provides broad composition flexibility as well as uniform microstructure.

Die compaction is a method to fabricate AMCs with a relatively low unit cost. However, the severe wear caused by higher percentages of hardening phase usually presents a problem. To prolong tooling life and improve the die compaction process, a top priority is to examine the fundamental mechanisms of wear and quantify the tool wear in die compaction of AMC powders to enable new practical solutions in industry.³

Numerous factors affect the die life. The punches and dies are in contact with each other as well as the metal

and hard particles, so the normal force, velocity, distance and lubrication, in combination with the large production quantities, lead to tool wear. The goal of this research was to develop a way to measure and quantify tool wear in die compaction of AMC powders and then determine the material constant in the proposed wear model. A combination of experimental and computational method was utilised to study the wear mechanisms in die compaction of AMC powders. Based on the analysis of experiment data, the possibility to predict tool wear by the simple wear model is discussed.^{5–9}

Theoretical background

Wear model

Based on Archard's law of wear,¹⁰ the authors propose the concept of wear work W_w by integration of frictional force multiplied by velocity with respect to time, given as follows

$$M_w = k \frac{W_w \rho}{H} = k \frac{\rho}{H} \int \mu N v dt \quad (1)$$

where M_w is the mass loss due to die wear, k is a wear material constant (depends on the powder composition), ρ is the density of tool material, H is the hardness of die material, μ is the friction coefficient between green compact and the die wall, N is the radial normal force, v is the average sliding velocity between the compact and the die wall and t is the testing time.

The mass loss M_w is obtained by direct measurement of the die, hardness H is measured on the HRC scale, time t was estimated by the approximate compaction rate of 70 compacts per minute and average compaction velocity was calculated by measuring compaction distance per cycle and dividing by the time.

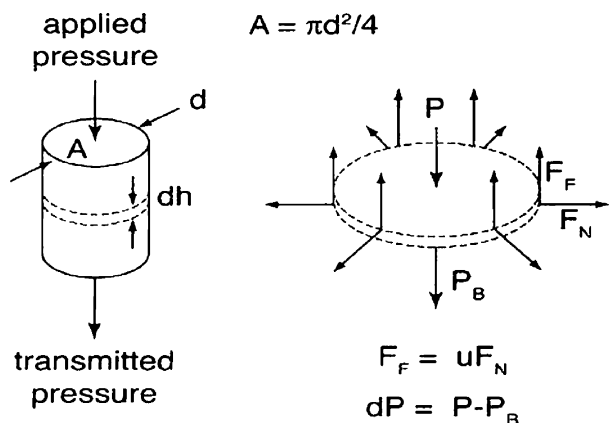
According to Kawata and Sugaya, the friction coefficient μ is ~ 0.8 for cemented carbide without lubricant.^{11–13} However, this high value is not in general agreement with other studies.^{14,15} Comparison of experimental data with and without the use of lubrication to that of finite element simulation using an iron

¹College of Engineering, San Diego State University, 5500 Campanile Drive, San Diego, CA 92182, USA

²Center for Advanced Vehicular Systems, Mississippi State University, 200 Research Boulevard, Starkville, MS 39759, USA

³Heraeus Incorporated, Materials Technology Division, 6165 W. Detroit Street, Chandler, AZ 85226, USA

*Corresponding author, email wei@cavs.msstate.edu



1 Force equilibrium in die compaction¹⁷

based powder resulted in a value of 0.1 for μ against the same WC die as the one used in the current study.¹⁶ Therefore, the authors assume that μ equals to 0.1 in all the calculations for convenient.

The product of μ and N equals to the friction force F_F between the compact and die wall. An indirect calculation method the friction force is introduced in the section on 'Friction force'.

Friction force

Friction force exists between the die cavity wall and the compact. It will not only lead to a pressure gradient along the compaction axis but also produce die wear. Die wall friction calculation in the present study was based on a simple free body force equilibrium relationship as shown in Fig. 1. The pressure distribution $P(h)$ within the compact was given as the following equation¹⁷

$$P(h) = P_A \exp\left(-\frac{4\mu v_e h}{d}\right) \quad (2)$$

where h is the compact height, d is the compact diameter, v_e is the dimensionless radial pressure ratio to applied pressure (effective poisson ratio) and P_A is the applied pressure at the top punch. When $h=0$, $P(h)=P_A$ and when h equals the total height of the compact h_t , $P(h_t)=P_B$, which is the actual compaction pressure at the bottom of the compact.

Friction force F_F can be calculated by the following equation¹⁷

$$F_F = \mu N = \pi \mu v_e dh (P_A - P_B) \quad (3)$$

The effective poisson ratio v_e and compaction pressure P_B are discussed in the sections on 'Model for elastic properties of porous material' and 'Compaction yield model' respectively.

Model for elastic properties of porous material

To determine radial normal force, Poisson's ratio as the ratio of applied axial pressure to the radial pressure is a necessary material elastic property. For the particulate reinforced AMC materials, as long as the hard particles are uniformly dispersed within the matrix, the assumption of isotropic properties is reasonable.

Mital *et al.*¹⁸ proposed that Poisson's ratio v_0 for dense isotropic particulate composite materials is given as

$$v_0 = \frac{E_{pc} - 2G_{pc}}{2G_{pc}} \quad (4)$$

where E_{pc} and G_{pc} are given by

$$E_{pc} = \frac{V_f^{0.67} E_b}{1 - V_f^{0.33} (1 - E_b/E_p)} + (1 - V_f^{0.67}) E_b \quad (5)$$

$$G_{pc} = \frac{V_f^{0.67} G_b}{1 - V_f^{0.33} (1 - G_b/G_p)} + (1 - V_f^{0.67}) G_b \quad (6)$$

where E is Young's modulus, G is shear modulus and subscripts pc, p and b represent particulate composite, particle (hard phase) and binder material (matrix) respectively. V_f is the volume fraction of the particles.

However, a porous structure usually has quite different material properties from that of bulk material. For porous structure, the Poisson's ratio depends on porosity. Assuming that the pores are spherical, according to the self-consistent theory proposed by Phani *et al.*,¹⁹ the effective Poisson's ratio v_e could be given as

$$v_e = \frac{2v_0(5v_0 - 7) + \theta(5v_0 - 3)(v_0 + 1)}{2(5v_0 - 7) + \theta(15v_0 - 13)(v_0 + 1)} \quad (7)$$

where θ is the porosity.

Compaction yield model

Understanding of the yield behaviour is very important for the study of compressibility of the powders. The Shima-Oyane model has been the most successful model for metal powders.²⁰ Based on this model, PMSolver²⁰ was used to determine a curve fit for experimental data of green density versus compaction pressure. Shima's model relies on a generalised form of the yield criterion, that is, yield surface $\Phi=0$, for compaction as

$$\Phi = \left(\frac{q}{\sigma_m}\right)^2 + \alpha(1-D)^\gamma \left(\frac{p}{\sigma_m}\right)^2 - D^m \quad (8)$$

where D is the relative density, q is the effective stress, p is the hydrostatic pressure, σ_m is the flow stress of the fully dense material and α , γ and m are material parameters. Parameters α , γ and m are determined by curve fitting yield stress data from uniaxial cylindrical compression tests over a range of relative densities. The flow stress σ_m of the fully dense material includes workhardening via a simple power law strain relation defined as follows

$$\sigma_m = a + b \bar{\epsilon}_m^n \quad (9)$$

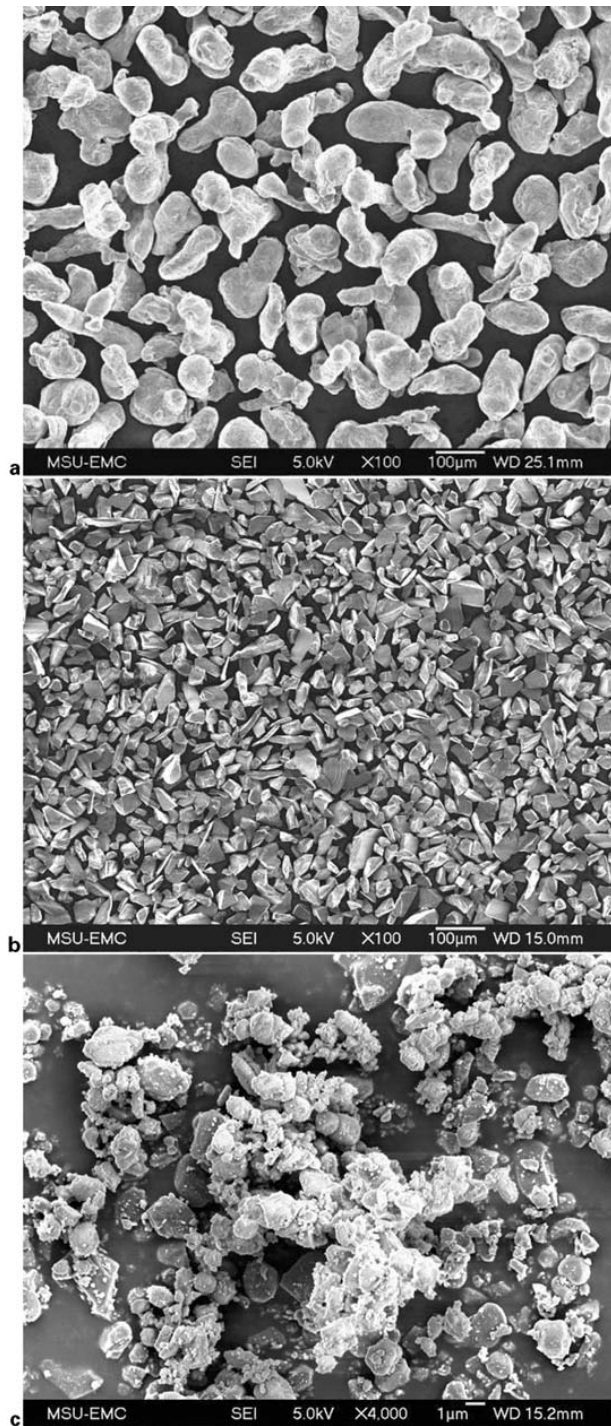
where a , b and n are material parameters and $\bar{\epsilon}_m$ is the effective strain of the fully dense material.²¹

Experimental

Materials

Powders

Air atomised Al alloy powder (AMB 2712, Ampal, Palmerton, PA, USA), SiC powder (SI-301, AEE, Bergenfield, NJ, USA) and Al₂O₃ powder (A2-325, Almatix, Bauxite, AR, USA) were used in this study. Particle size distributions were measured using a laser particle size analyser (LA-950, Horiba Instruments, Irvine, CA, USA). The SiC particles are larger and harder than the alumina particles. The powder characteristics are listed in Table 1. In practice, the SiC and Al₂O₃ powders are mixed with the Al alloy powder to form a composite. Scanning electron microscopy (SEM; Zeiss, Stereoscan 360) images of the powder particles are



a Al alloy; b SiC; c Al₂O₃

2 Scanning electron microscopy images of powders

given in Fig. 2. The hardness for powder materials comes from Cambridge Engineering Selector, Material Universe database,²² as listed in Table 1.

Table 1 Powder characteristics

Powder	Al alloy (AMB 2712)	SiC (SI-301)	Al ₂ O ₃ (A2-325)
Vendor	Ampal	AEE	Almatis
Composition	Al-3.8Cu-0.75Si-1.0Mg	SiC	Al ₂ O ₃
D ₁₀ , µm	52.9	6.8	0.3
D ₅₀ , µm	77.7	9.2	1.8
D ₉₀ , µm	110.9	13.6	4.5
Pycnometer density, g cm ⁻³	2.71	3.22	3.93
Hardness, HV	80	2380	1860

Table 2 Tested powder mixtures experiment design

ID	Hard additives			Lubrication
	Type	wt-%	vol.-%	wt-%
CP 1	SiC	5	4.3	0.4
CP 2		10	8.6	
CP 3		15	12.9	
CP 4	Al ₂ O ₃	5	3.5	0.4
CP 5		10	7.1	
CP 6		15	10.9	
CP 2	SiC	10	8.6	0.4
CP 7				0.8
CP 8				1.2

Die material

Tungsten carbide-cobalt BC-14S containing 14%Co (Basic Carbide, Lowber, PA, USA), with the density of 14.06 g cm⁻³ and HRC of 78.1 ± 0.3 was used as die material.

Lubricant

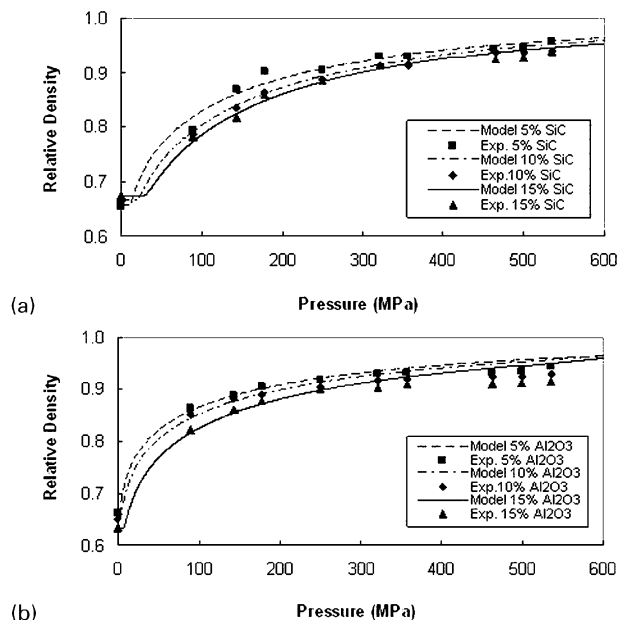
The AMB 2712 aluminium alloy used in the present study only has 0.75 wt-%Si, which makes it less abrasive than an alloy of higher Si content. However, the SiC and Al₂O₃ reinforcement particles make the composite powder mixtures abrasive. To reduce the tool wear, 0.4–1.2 wt-% of Acrawax C (Lonza Ltd, Basel, Switzerland) was chosen as a premixed lubricant. The particle size of lubricant powder ranges from 45 to 106 µm.

Die wall lubricant (Zinc Stearate Dry Powder Mould Release, Aervoe Industrial Inc., Gardnerville, NV, USA) was applied to the die wall to generate a near frictionless state as one of the known boundary conditions for pressure distribution model described by equation (2).

Compaction

The Al-SiC and Al-Al₂O₃ powder mixtures with different lubricant levels were compacted using a Carver Hand Press (Model M, hydraulic unit model 3925) and an industrial tablet press (Stokes Model F, 4 ton Mechanical Press). The hand press was used to make larger cylindrical compacts for powder compressibility characterisation, while the tablet press was used for automatic compaction to study the die wear. A verification study of the hand press showed that pressure measurements were accurate to within ± 7 MPa.

Powder mixtures of eight different compositions were used in the hand press and automatic compaction experiments, from which hard phase content effect, hard phase type effect as well as the lubricant level effect could be determined. Information about powder mixtures and experiment design is given in Table 2.



(a) Al-SiC system, CP 1, CP 2 and CP 3; (b) Al-Al₂O₃ system CP 4, CP 5 and CP 6

3 Compressibility of AMC powder mixtures with 0.4 wt-% lubricant

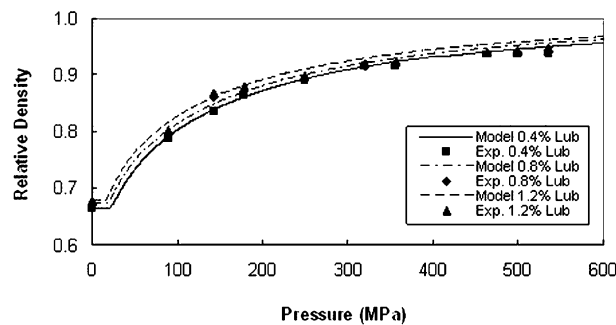
The tablet press used for automatic compaction experiment had no capability to read the applied pressure. Compressibility information enabled the determination of the applied pressure during automatic compaction from the measured compact density.

Compressibility

Cylindrical compacts of 12.75 mm diameter of the Al-SiC and Al-Al₂O₃ powder mixtures with 0.4 wt-% lubricant were compacted using manual press. Die wall lubricant was applied to minimise the friction effect along the die wall. The compact weight was controlled to 2.5 ± 0.2 g. Because the powder was filled into the die cavity by hand, any operation error during powder filling process may result in the compact mass variation. Pressures in the range of 89–535 MPa were used to produce at least three compacts for each pressure. The green densities of the compacts were calculated using mass and dimensions of the compacts. The mass scale was calibrated using multiple measurements of a 10 g mass standard, and its accuracy was ± 0.0008 g. The vernier caliper accuracy was ± 0.01 mm.

Die wear

The automatic compaction experiment was used to simulate the industrial production process. The top and bottom punches were made from M4 tool steel. Wear



4 Compressibility of 90Al-10SiC powder mixtures with various lubricant levels, CP 2, CP 7 and CP 8

from compaction of the Al-SiC and Al-Al₂O₃ powder mixtures were measured on the tungsten carbide BC-14S die. Cylindrical compacts with diameters of 6.35 mm and heights of ~ 4.5 mm were compacted at a rate of ~ 70 compacts/min. The bottom punch was adjusted to hold a filling height of 7.8 mm. The upper punch stroke length was calibrated to achieve green compact relative densities of $80 \pm 1\%$ theoretical. For each of the powder mixture composition, 30 000 samples were compacted.

Applied pressure P_A and bottom pressure P_B for all compositions are listed in Table 3 (note that the relative green density includes the lubricant). However, the natural powder fill variation results in a green density and peak pressure variation.

Results and discussion

Compressibility

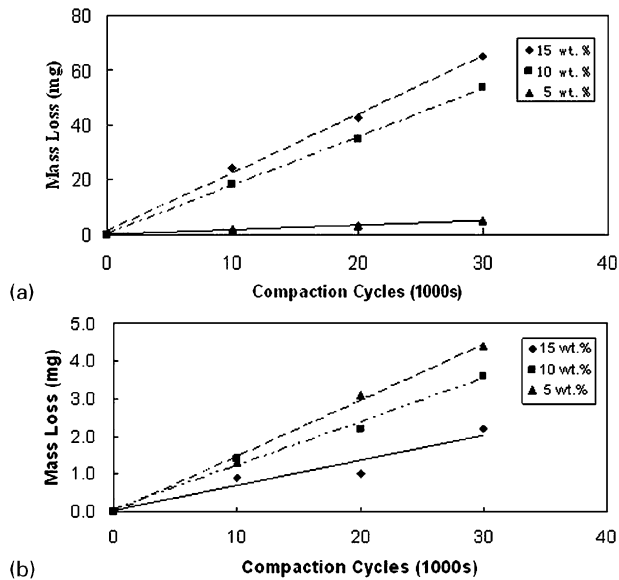
Figure 3 shows the hard particle effects on compressibility of the AMC powder mixtures. Curve fits of the green density data were generated by PMSolver and included in these plots. Since die wall lubrication was applied for all compressibility compaction experiments, it was assumed that the die wall was frictionless. The model assumed early stage rearrangement before deformation.

Figure 4 shows the lubricant content effects on the compressibility of AMC powder mixtures.

The compressibility curves show the typical trend of an asymptotic increase in density as the compaction pressure increases, and the reduced compressibility was observed as the content of hard phase (SiC or Al₂O₃) increases. For the current powders, it was found that Al-SiC powder mixtures are harder to compress than Al-Al₂O₃ powder mixtures. Admixed lubricant did improve the compressibility of the 90Al-10SiC powder mixture. The maximum lubricant content, 1.2 wt-%, resulted in the best compressibility. The relative density

Table 3 Compaction parameters for all compositions

	ID	Effective ν	Rel. ρ	P_A , MPa	P_B , MPa	Compaction ratio
Al-SiC	CP 1	0.375	0.81	112.8	81.6	1.70
	CP 2	0.368	0.80	134.7	97.4	1.66
	CP 3	0.361	0.79	142.0	104.0	1.70
Al-Al ₂ O ₃	CP 4	0.378	0.82	68.3	50.0	1.77
	CP 5	0.372	0.80	65.3	48.4	1.81
	CP 6	0.355	0.72	36.3	27.3	1.81
Al-SiC	CP 2	0.368	0.80	134.7	97.4	1.66
	CP 7	0.366	0.79	108.3	79.0	1.70
	CP 8	0.366	0.79	93.8	68.4	1.70



a Al-SiC system, CP 1, CP 2 and CP 3; b Al-Al₂O₃ system, CP 4, CP 5 and CP 6

5 Die mass loss v. compaction cycles

curve fit using the Shima–Oyane model fits the experimental data points within 0.5% average difference at pressures below 300 MPa. Overestimation of density from the model was observed at pressures higher than 300 MPa. An explanation might be that the hard–soft particle mixture probably requires a shift in treatment as the density increases since, at low densities, the soft particles deform; yet at high densities, the hard particles have never deformed but contributed to faster work hardening (than typical) of the soft particles.

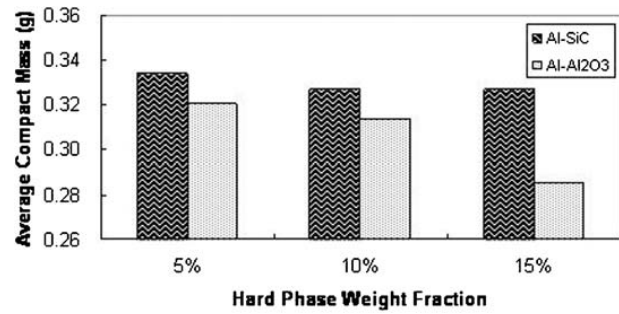
Based on these compressibility data, the applied pressure in equation (2) can be determined and the friction force calculated (equation (3)).

Die wear

Die mass loss and k value were chosen as two major criteria for the comparison of wear behaviour of powder mixtures in the present study. Die mass loss is related to the geometry change of the die cavity. For example, more mass loss means bigger enlarged die cavity diameter because material was removed by friction. Thus, mass loss is aimed to be minimised. The wear material parameter k is related to dimensional change of a die, which is used to press specific powder mixtures under a given compaction cycles (or friction work). Therefore, the wear material parameter k (cm³ HRC kJ⁻¹) could be interpreted as the cavity volume change of the die due to per kilojoules friction work. However, each k value only corresponds to powder system, and it is independent of die hardness. Before determining the wear material parameter k , the wear work W_w in equation (1) was calculated using results from equation (3).

Figure 5 shows the die mass loss evolution versus compaction cycles using Al-SiC and Al-Al₂O₃ powder mixture systems with 0.4 wt-% lubricant. Note that the behaviour is linear with compaction cycles. Comparison of hard particle effects on wear model parameters is listed in Table 4.

From the data shown in Table 4, the authors found that, for Al-SiC compositions, higher SiC content leads to more die mass loss, while for Al-Al₂O₃ compositions,



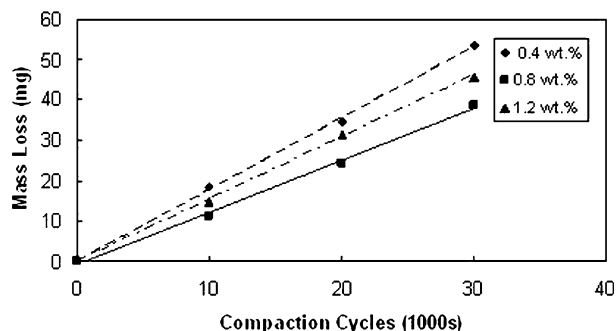
6 Average compact mass v. fraction of hard phase

an opposite trend was observed (note that all the Al-SiC powder mixtures produced much higher die mass loss comparing to that produced by Al-Al₂O₃ powder mixtures.) Therefore, besides the hard phase content and hardness, many other factors also seem to play important roles in the wear behaviour during die compaction.

After analysing the powder characteristics, differences among particle size, particle shape as well as the powder flowability are found to be the most likely reasons for different wear behaviour of different powders. As pointed out by German, powder flowability is dependent on particle size, particle shape as well as particle surface roughness.¹⁷ Generally, larger particle size and sphere particle shape lead to better flowability, while smaller particle size and irregular particle shape result in worse flowability. According to SEM images of powders, the SiC particle size was about 10 times that of the Al₂O₃ particle; moreover, the larger SiC particles have more irregular shape with sharp edges, while the finer Al₂O₃ particles are near spherical. However, among particle size and particle shape, which factor plays a more important role in the powder flowability property? Although no flowability tests were conducted to compare the two powder systems (Al-SiC and Al-Al₂O₃) quantitatively, it was easy to notice that the Al-SiC powder mixtures showed better flowability than the Al-Al₂O₃ powder mixtures during the filling stage. As shown in Fig. 6, average Al-SiC compact weights are heavier than those of Al-Al₂O₃ compacts with the same hard phase content. The flowability decreasing trends were also observed for 5, 10 and 15 wt-%SiC and Al₂O₃ additions. With increasing amount of hard phase content, the amount of powder filled in the die during automatic compaction was lower (compact was lighter). Under the same preset top punch compaction distance, higher applied pressure would be generated within the die cavity, which was filled with more powder, and higher friction force (more wear) follows higher applied

Table 4 Hard particle effects on wear parameters

ID	Effect	M_w , mg	W_w , kJ	k , cm ³ HRC kJ ⁻¹
CP 1	SiC	4.9	261.6	0.104×10^{-6}
CP 2		53.5	307.9	0.962×10^{-6}
CP 3		65.1	319.0	1.130×10^{-6}
CP 4	Al ₂ O ₃	4.4	158.9	0.153×10^{-6}
CP 5		3.6	149.5	0.133×10^{-6}
CP 6		2.2	79.9	0.153×10^{-6}
CP 2	Lubricant	53.5	307.9	0.962×10^{-6}
CP 7		38.8	246.2	0.873×10^{-6}
CP 8		45.7	213.2	1.190×10^{-6}



7 Lubricant effects on mass loss of die v. compaction cycles, CP 2, CP 7 and CP 8

pressure always. This is how the powder flowability affects the die wear. In the current study, the particle size plays a more significant role than particle shape in affecting the powder flowability.

Besides the flowability, particle shape itself also affects the die wear. Compact pressed from particles with more irregular shape will form rougher surface, which will result in more wear on the die. This might be another important reason that Al-SiC powder mixtures generated more wear on the die than Al-Al₂O₃ powder mixtures.

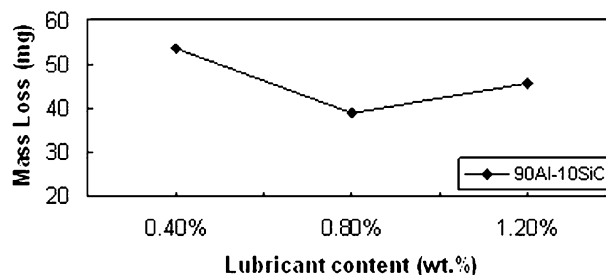
Based on the discussion above, the authors conclude that for Al-SiC powder mixtures, particle shape and hard phase content played more important roles in affecting the die wear than powder flowability because with increasing the SiC content, more die wear was observed. For Al-Al₂O₃ powder mixtures, powder flowability contributed more in affecting die wear than hard phase content because with increasing the Al₂O₃ content, lighter compact weight and less die wear were observed.

Figure 7 indicates the die mass loss versus compaction cycles using 90Al-10SiC powder mixtures with different lubricant levels, while Fig. 8 shows the total mass loss of the die for the three powder compositions with different lubricant contents. Table 4 compares the lubricant effects on constants of wear model.

Note for compositions of different lubricant levels, a near V shape trend was observed in the plot of total mass loss v. lubricant content. This means that the intermediate lubricant level could be the optimum condition for reducing die wear. However, the reason behind this behaviour is not clear. In this current study, it was observed that higher lubricant content led to better powder flowability (helping to granulate the powder into bigger agglomerated round particle). Therefore, under the same top punch compaction distance, higher pressure was generated. It might be the reason why the powder with the highest lubricant level produced higher wear in the current case.

To predict a more realistic trend of lubricant effect, the result in Fig. 8 needs further expansion to higher lubricant level.

The authors' model assumed that wear is due to the relative motion of powders and die wall during compaction and ejection. Therefore, the abrasion wear was considered as the dominant wear mechanism. In agreement, Figs. 5 and 6 show that near linear relationships between mass loss and compaction cycles were observed. This indicates that the proposed wear model



8 Lubricant effects on total mass loss of die after 30 000 cycles

can properly explain the wear within the present compaction cycle range for the die. The material constant k is the slope of the straight line because wear work is a linear function of compaction cycles. Moreover, one important fact that needs to be considered is that k is only dependent on the powder (composition and geometry), which is being compressed in the rigid die, and k is independent of die materials. This fact has been studied and proved by the authors in another paper titled 'Tribological behaviour of die tool materials used for die compaction in powder metallurgy', which is a collaboration research with Blau *et al.* from the High Temperature Material Lab under Oak Ridge National Laboratory. The second paper will be published in *Powder Metallurgy*.

Conclusion

In automatic die compaction, measurement of mass loss proved to be an effective means to characterise die wear. For AMCs, a linear relation exists between die mass loss and the number of compaction cycles. This indicates that the proposed modified Archard's law can describe the wear mechanism properly within the 30 000 compaction cycles range studied here. Material related factors, including hard phase content, hard particle material, hard particle shape, hard particle size distribution as well as lubricant level, all were found to have influences on tool wear. Process related factor, compaction pressure, is another important factor that is able to affect the die wear as well.

Acknowledgements

The authors would like to thank the Department of Energy, USA, for funding this project (award no. DEFC2606NT42755), Ampal Inc. for providing the aluminium powder, and Lonza Inc. for providing Acrawax C lubricant.

References

1. Y. Pan, Z.-Q. Gao and G.-X. Sun: *J. Southeast Univ.*, 1993, **23**, (Suppl.), 142-146.
2. H. R. Hafizpour and A. Simchi: *Powder Metall.*, 2008, **51**, (3), 217-223.
3. D. Daubert: 'Preventing PM-compaction failure', *Am. Mach.*, 1977, **121**, (8), 93-95.
4. G. O'Donnell and L. Looney: *Mater. Sci. Eng. A*, 2001, **A303**, 292-301.
5. J. J. Lewandowski, C. Liu and W. H. Hunt, Jr: 'Processing and properties for powder metallurgy composites', 117-137; 1988, Warrendale, PA, The Metallurgical Society.
6. A. V. Krajinov, M. Gastel, H. M. Ortner and V. V. Likutin: *Appl. Surf. Sci.*, 2002, **191**, 26-43.
7. A. Pohl: *Powder Metall.*, 2006, **49**, (2), 104-106.

8. G. B. Schaffer: *Mater. Forum*, 2004, **28**, 65–74.
9. I. E. Anderson and J. C. Foley: *Surf. Interf. Anal.*, 2001, **31**, 599–608.
10. K. C. Ludema: 'Friction, wear, lubrication: a textbook in tribology'; 1996, Boca Raton, FL, CRC Press.
11. Y. Sugaya: 'Research on structure of compacting die for reducing ejection force of green compact', Hitachi Powdered Metals Technical Report, Vol. 6, 12–20; 2007, Tokyo, Hitachi Powdered Metals.
12. K. Kawata: 'Application to the metallic mold of the various hard films deposited by the plasma CVD methods', *Molds Technol.*, 1999, **14**, (5), 65–71.
13. K. Kawata: *Surf. Technol.*, 2002, **53**, (11), 28–29.
14. Sh. Keshavarz, A. R. Khoei and A. R. Khaloo: *Mater. Des.*, 2008, **29**, 1199–1211.
15. D. T. Gethin and R. W. Lewis: 'Finite element modeling of powder compaction and its experimental validation', Proc. Powder Metallurgy World Cong., Paris, France, June 1994, EPMA, 689–692.
16. Y.-S. Kwon, S.-H. Chung, K. T. Kim, R. M. German and H. I. Sanderow: 'Numerical analysis and optimization of die compaction process', in 'Advances in powder metallurgy and particulate materials', Part 4, 4-37–4-50; 2003, Princeton, NJ, MPIF.
17. R. M. German: 'Powder metallurgy and particulate materials processing', 181–186; 2005, Princeton, NJ, MPIF.
18. S. K. Mital, P. L. N. Murthy and R. K. Goldberg: 'Micromechanics for particulate reinforced composites,' NASA Technical Memorandum 107276; 1996, Washington, DC, National Aeronautics and Space Administration.
19. K. K. Phani and D. Sanyal: *J. Mater. Sci.*, 2005, **40**, 5685–5690.
20. S. Shima and M. Oyane: *Int. J. Mech. Sci.*, 1976, **18**, 285–291.
21. Cetatech: 'Theoretical background – PMSolver', User Manual; 2006, Sacheon, Cetatech.
22. Granta Design Ltd: 'Cambridge engineering selector (CES EduPack 2007)', Level 3, Material Universe Database; 2007, Cambridge, Granta Design Ltd.

Authors Queries

Journal: **Powder Metallurgy**

Paper: **1530**

Title: **Investigation on die wear behaviour during compaction of aluminium matrix composite powders**

Dear Author

During the preparation of your manuscript for publication, the questions listed below have arisen. Please attend to these matters and return this form with your proof. Many thanks for your assistance

Query Reference	Query	Remarks
1	Author: Please confirm the running head.	
2	Figures 1–8 are low quality, please supply a higher resolution version if possible.	